EXTERNAL STORE SEPARATION FROM FIGHTER AIRCRAFT

H. Özgür DEMİR
Aerospace Engineering Dept.
Middle East Technical University
06531 Ankara TURKEY

odemir@ae.metu.edu.tr

Prof. Nafiz ALEMDAROĞLU
Aerospace Engineering Dept
Middle East Technical University
06531 Ankara TURKEY

nafiz@metu.edu.tr

Vahit ÖZVEREN
ASELSAN A.Ş. MST
P.O. Box 101, Yenimahalle
06172 Ankara TURKEY

vozveren@aselsan.com.tr

ABSTRACT

This paper presents the results obtained for store separation from an aircraft by CFD methods. The computational results are validated against the available experimental data of a generic wing-pylon-store configuration at Mach 0.95. Two different commercially available CFD codes; CFD-FASTRAN an implicit Euler solver and an unsteady panel method solver USAERO, coupled with integral boundary layer solution procedure are used for the present calculations. CFD-FASTRAN is validated against the experimental data of Eglin generic wing-pylon-store configuration at Mach 0.95. Major trends of the separation are captured. Similar configuration is used for the comparison of unsteady panel method with Euler solution at Mach 0.3 and 0.6. Displacements, angular orientations, pressure coefficient distribution on the store in captive position and force coefficients histories during separation are used for comparison. Major trends are similar to each other while some differences in lateral and longitudinal displacements are observed. Finally, separation of a fuel tank from an F-16 aircraft wing and full aircraft configurations are solved at Mach 0.3 using the unsteady panel code only. In this case, the effect of the fuselage is observed on the trajectories and angular orientations of the fuel tank. The results and advantages of the two codes for solving the store separation problem from air platforms are discussed in detail.

1.0 INTRODUCTION

Safe separation of a store from an aircraft is one of the major aerodynamic problems in the design and integration of a new store to an aircraft. Carriage loads and moments acting on the store should be correctly predicted in order to have an idea about its separation behavior. It is difficult to predict correctly the aircraft flow field especially in the transonic regimes since the flow field is highly dominated by shocks. Also, the interaction between the store and the pylon affects the attitude of the store after its release. Therefore, time consuming and costly wind-tunnel and flight tests are needed in order to obtain the necessary carriage and trajectory data. Since computational methods for the trajectory calculations give reliable data with less time and cost, they are used before and after the wind tunnel and flight tests to obtain the optimum integration and separation configurations for the store.

The purpose of this study is to demonstrate some of the capabilities of the computational prediction tools. Two separate computational tools are used; CFD-FASTRAN, an inviscid Euler solver with chimera overlapping grid technique and an unsteady panel method solver, USAERO, coupled with the integral

Paper presented at the RTO AVT Symposium on "Functional and Mechanical Integration of Weapons and Land and Air Vehicles", held in Williamsburg, VA, USA, 7-9 June 2004, and published in RTO-MP-AVT-108.

boundary layer method. These codes are used to obtain the unsteady trajectory characteristics of a store released under subsonic flow conditions. The results are presented in terms of store trajectory, angular orientations and pressure distribution on the store in captive position.

Chimera technique is very often used for relative body motions. CFD-FASTRAN is one of the codes that use implicit Euler/Navier-Stokes flow solver with chimera overlapping grid technique for relative body motion problems. This code is validated for the Eglin Test Case once and the results are presented in Ref. [1] and a similar technique of solution was further used to validate the simulation of a jettisoned aircraft canopy trajectory [2]. Also JDAM separation results from an F-18 aircraft are also published in Ref [3].

USAERO, a time-stepping panel method coupled with a wake model and thin boundary layer assumption with Flight Path Integrator (FPI) module, is the other code used for the present store separation problem. Since the modeling and the solution time of a panel code is considerably less than that of the Euler solutions, panel codes are frequently used as an engineering tool in achieving practical objectives [4]. Same configuration without the sting attachment to the store is solved at Mach numbers of 0.3 and 0.6, with the USAERO code.

Two different wing-pylon-store configurations are solved. The first one is the well-known Eglin wing-pylon-finned store test case and is solved with the CFD-FASTRAN solver at a Mach of 0.95. There are several reports that successfully predict the trajectory characteristics of this problem [5-7]. The results of the present computations are compared with the available experimental and computational data. It is observed that all of the major trends of the trajectory for this particular problem are captured with the present Euler solution technique.

The next case solved is the same Eglin configuration at two different Mach numbers; Mach 0.3 and 0.6. Both codes are used to predict the trajectory and the orientations of the store in its trajectory. As a final test case, the separation of a fuel tank from an F-16 fighter aircraft's wing-pylon configuration and a full F-16 aircraft configuration are also demonstrated with the use of USAERO unsteady panel code.

Unfortunately, no experimental data are available for Mach 0.3 and 0.6 cases for both the Eglin and the fuel tank separation from F-16 aircraft for comparison purposes. However, it is believed that the present results could be used to demonstrate the capabilities of both of these codes and their applicability for store separation studies.

2.0 CONFIGURATIONS

In this study, three configurations are used to demonstrate the applicability of the CFD codes to store separation problems. The general coordinate system is given in Figure 1. The origin is located at the c.g. location of the store at its captive position. Phi, theta and psi angles represent rotation towards outboard around the x-axis (roll), upwards around the y-axis (pitch) and towards the outboard around the z axis (yaw), respectively.

2.1 Eglin Wing-Pylon-Finned Store Validation Test Case

The well-known Eglin test configuration [8] is given in Figure 1. Store geometry is modeled with the sting, same as used during the experiments. The detailed geometry definitions can be found in References [5] and [8]. Experimental data for this test case is available at both M=0.95 and M=1.2. In this study, only the M=0.95 case is considered.

2.2 Eglin Wing-Pylon-Finned Store, M=0.3, M=0.6

This configuration is the same as the Eglin test case except that the sting is not used and the store is cut through the sting attachment location (Figure2). This case is tested with both codes in order to have an idea about the results of the forces acting on the store and the calculated trajectories. Base-cut configuration is preferred rather than a smooth revolved store base since in order to have a reasonable drag value, the separated flow must be modeled using a *base wake* in USAERO panel code. The ejector forces are kept the same as is used in the original validation test case.

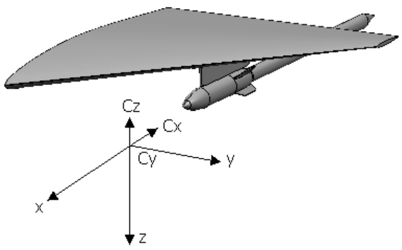

Figure 1: Coordinate Axis System
(Eglin Test Case Configuration)

Figure 2: Eglin Configuration without Sting

2.3 F-16 Fighter Aircraft Wing / Full Configuration Cases

The surface geometry of F-16 aircraft and the fuel tank drawings are shown in Figure 3. The wing geometry was extracted from the full F-16 geometry for wing alone case. Root section of the wing is extruded until the symmetry plane of the aircraft in order to diminish the strong compressed flow region between the symmetry boundary condition and the store. In its captive position, fuel tank has a negative angle of attack of 3^0 due to installation.

The aim of this F-16 aircraft solution with an unsteady panel code is to investigate if there is a large fuselage effect which contributes to the separation phenomenon. Since there is no experimental data available for this study, the choice of the weight and ejector forces may be unrealistic. However, the choice of these parameters is not very significant since the aim of this case study is to investigate the fuselage effect on the store trajectory.

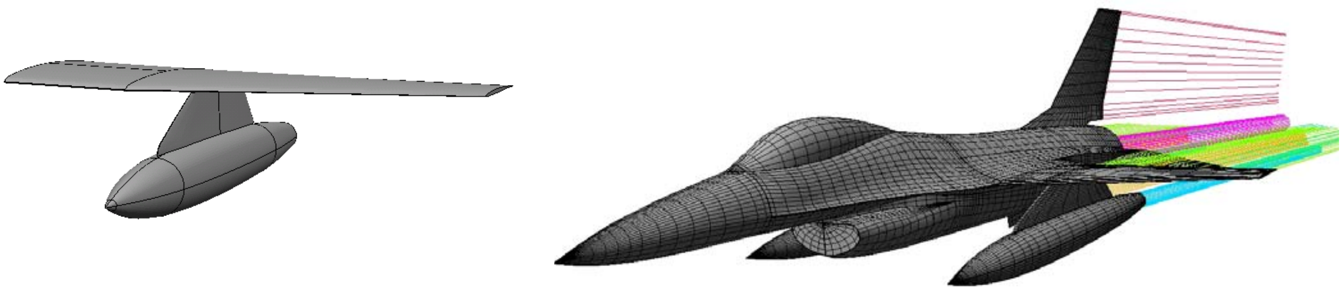

Figure 3: F-16 Wing/Pylon/Fuel tank (left) and Full Aircraft Configuration

The fuel tank geometry closely resembles that of the 370 gallon external fuel tank geometry without the fins. Engine inlet boundary condition data is obtained from the previous studies done in the Aerospace Engineering Department of METU [9-10]. The mass of the fuel tank is taken as 250 kg as if it is nearly empty before the separation. Moment of inertia calculation is done by the code USAERO itself, by assuming that the given mass value is evenly distributed over the entire store. The c.g. location of the fuel tank is chosen at the mid point location of the longitudinal axis passing from the nose of the store. The ejector forces applied to the store are placed at 15 cm. aft and forward of the c.g. location, with values of 4000 N and 6000 N respectively.

3.0 GRID TOPOLOGY & PANELLING

3.1 Euler Mesh for CFD-FASTRAN

Volume mesh for the Euler solutions is generated with CFD-GEOM; the pre-processor of CFD-FASTRAN. The wing and the pylon geometries are immersed in an H type grid using multi-block grid technique (Figure 4). Wing-pylon volume mesh is built up with 13 blocks having a total of 900000 cells. Connectivity between the blocks is supplied by interface boundary condition. The store is meshed alone for the chimera purposes. O-type grid topology is used for the store domain, and is built up with 16 blocks and 230000 computation cells. Two domains are overlapped using CFD-GEOM by simple cut and paste technique. Initial and boundary conditions, solution type and techniques are input by using the CFD-FASTRAN graphical user interface. The outer boundary of the store domain is set as the overset boundary condition (Figure 5).

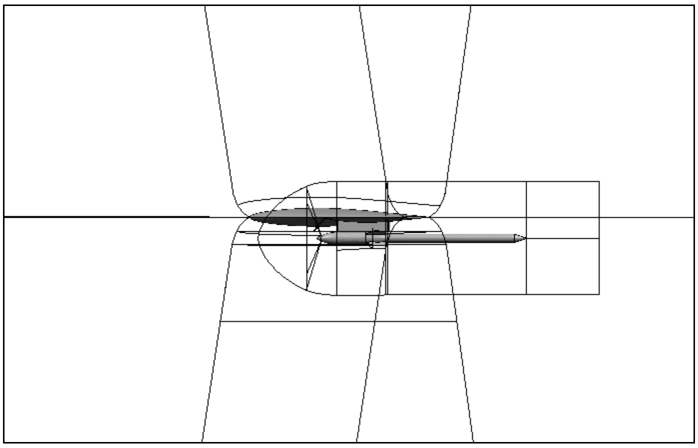

Figure 4: Eglin Test Case Grid Topology with Overlapping Store Grids

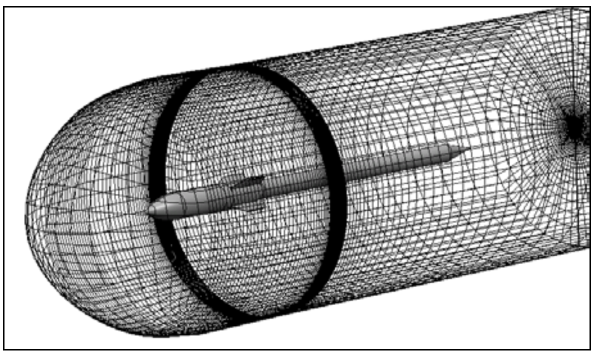

Figure 5: Store Computational Domain, Overset Boundaries

3.2 Paneling for USAERO

The surface paneling for USAERO code is also created using the CFD-GEOM software. The surface panels are then exported to a compatible format for USAERO using a FORTRAN code. The surface panel warp and surface normal directions are checked and corrected with SPIN(g), the pre-processor of USAERO. Other modifications such as ordering, splitting, and joining of panel groups (patches) are also performed using the SPIN(g). For free shear layer simulation, a wake model is also introduced using the other pre-processor, SPIN(w) of USAERO. 2712 body panels are used to model the Eglin configuration (Figure 6) where as 4117 and 6046 body panels are used to model F-16 wing-pylon-fuel tank and half of the F-16 full aircraft configurations (Figure 7), respectively.

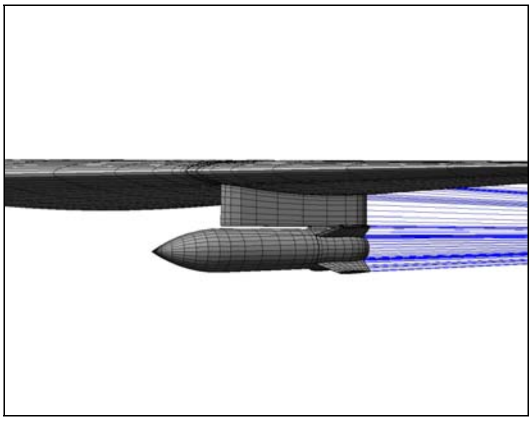

Figure 6: Paneling of Eglin Configuration

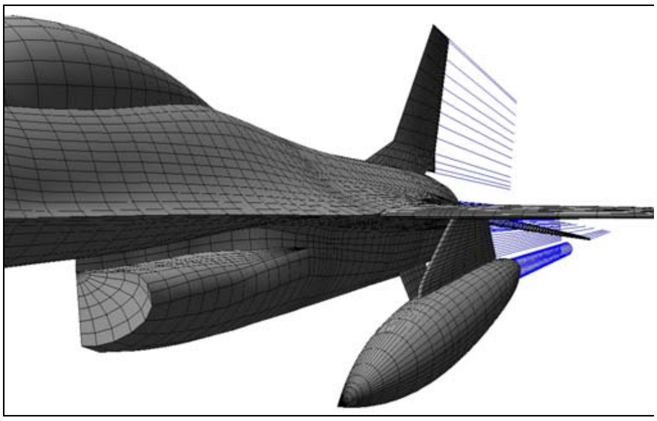

Figure 7: Paneling of F-16 Aircraft with Fuel Tank

4.0 COMPUTATIONS

Steady-state and implicit Euler solutions are obtained before the time accurate computations started. Roe's approximate Riemann solver scheme is used for flux computations, which is first order spatially accurate. Second order accuracy is obtained using Minmod (1/r) limiter. CFL number is increased from 1 to 20 in 200 iterations for steady-state calculations. Time step is taken as 0.00005 for the transient computations. CPU computation time for 1 time step takes an average value of 156 s using a P4 2 GHz stand-alone computer. 5700 time step solutions take maximum of 1.9×10^5 CPU time using a parallel computing cluster built up with 16 PIII 733 MHz CPUs. The domain decomposition in structured grids for parallel computations is performed by assigning of blocks to different CPUs. Therefore, the blocks must be created nearly of the same size in order to obtain a well balanced, equally loaded distribution.

A time step of 0.001 is used for the unsteady panel code solutions. 30 time steps are used in order to establish the wake before the separation process starts. Viscous effects are taken into account by activating the boundary layer coupling with potential flow solution. A direct matrix solver, LAPACK, is used for the matrix inversions. Solutions are obtained using a SGI Octane stand-alone computer. The average CPU time needed for 2712 surface panels with wakes is 106 seconds. The first time step takes a CPU time (without wakes) of 22.67 seconds and the last time step takes 208.80 seconds. F-16 aircraft configuration with 6046 body panels takes 20 hours of CPU time.

Both programs have its own 6DOF code embedded in the main solver. There are two main differences observed in the modeling of 6DOF. First difference is about the wall boundary selection, which will be used for the 6DOF. In USAERO, all geometry assigned to the FPI frame (either directly or indirectly) will contribute to the aerodynamic forces/moments used in 6DOF calculations [11]. Therefore, the forces and moments acting on the sting attached to the store also contribute to the separation process directly. In CFD-FASTRAN, sting also moves with the store while the forces and moments acting on the sting are excluded from the aerodynamic force and moment calculations. Second difference is about the ejector modeling. The ejector launch simulation is simplified by assuming that the direction of the force relative to the aircraft coordinate axis does not vary with time and that the point on the store where the force act does not change with time in USAERO [8]. If the point forces application locations are given with respect to the inertial frame, the application points on the store change with time in CFD-FASTRAN code.

5.0 RESULTS

5.1 Eglin Test Case, M=0.95

Eglin test case [8] is solved using CFD-FASTRAN with overlapping grid methodology. The results given below represent the linear and angular displacements as well as the velocities and pressure distributions on the store at four different angular positions and the time history of the force coefficients. It is observed that all of the major trends are captured when one compares the results with those given in Ref [5].

Store moves towards inboard and backwards while moving down with the effect of gravity and the ejector forces after its release. Total forces acting on the store result in a pitch up, yaw and roll to the outboard motion (Figure 8). Aerodynamic forces acting on the store result in a pitch down moment [5], which can be seen after the vanishing of the ejector forces effects. The effect of the ejector forces can be clearly seen from Figure 9. The angular pitch rate starts to decrease after t=0.05 s, corresponding to the end of the stroke. The discrepancy between the velocity data and the results obtained increases after t=0.2 seconds due to the differences in angular orientations [5]. This difference also affects the force coefficients history as seen in Figure 11. Although there are small discrepancies between the present results and the experimental data, it is observed that the general trends for all the curves are captured.

Figure 10 shows the pressure coefficient distribution on the store at the captive carriage position (t=0). Interaction effects between the store and the pylon can be seen from these graphs. Phi=5 degree cut plane location is in the gap region between the pylon and the store. The compression due to pylon is also captured. However, the expansion after the compression is under predicted. Outboard yawing moment tendency of the store can be predicted from the pressure coefficient distribution graphs at Phi=95^0 and Phi=275^0 locations. Shock locations are also well predicted.

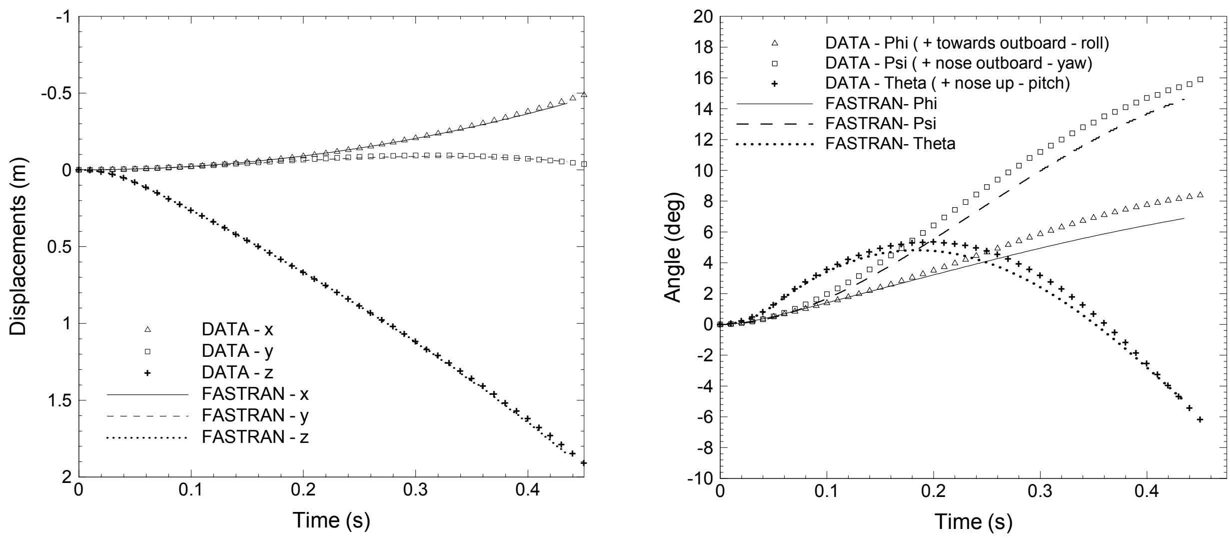

Figure 8: Linear and Angular Displacements, Eglin Validation Test Case, M=0.95

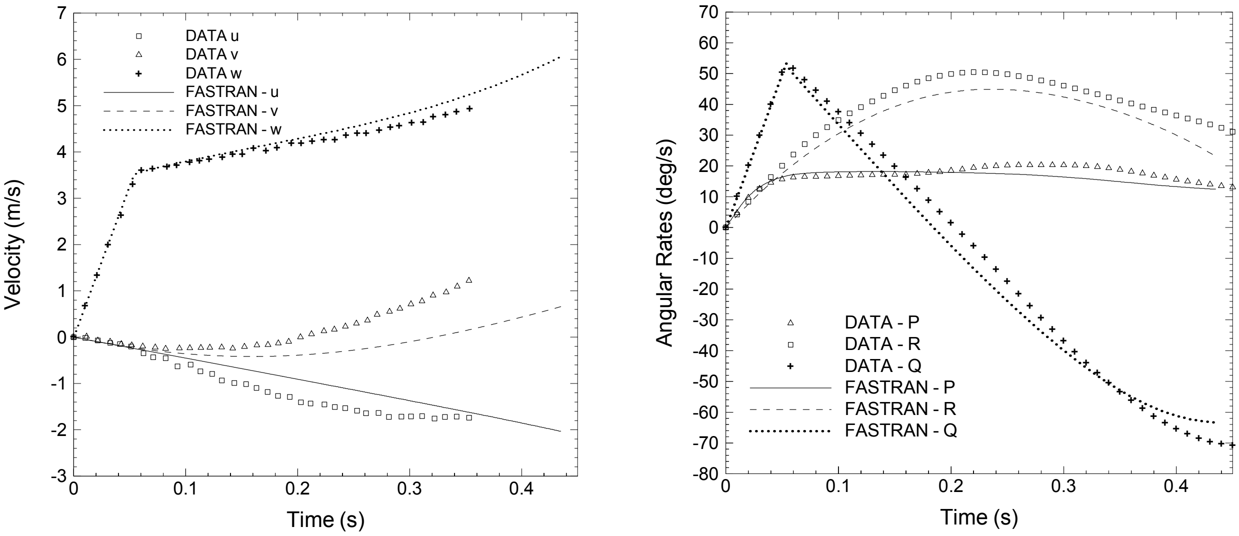

Figure 9: Linear and Angular Velocities, Eglin Validation Test Case, M=0.95

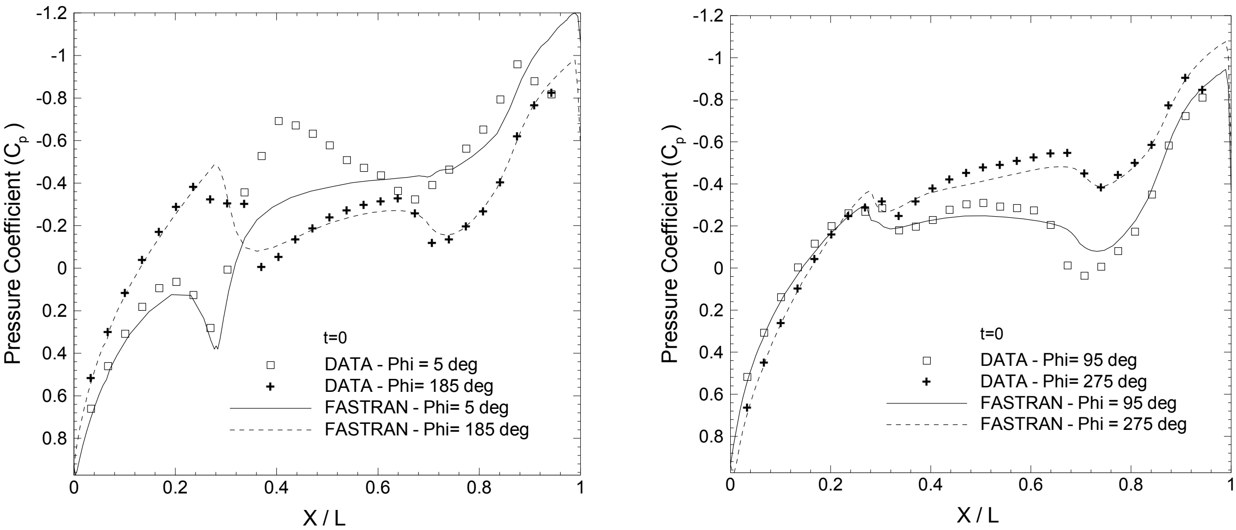

Figure 10: Pressure Distribution on the Store in Captive Position, Eglin Validation Test Case, M=0.95

Time histories of the force coefficients graph are given in Figure 11. Cx graphs are drawn with and without the base pressure correction. The displacements are obtained with the base pressure correction applied to the store. Otherwise, the drag on the store would be higher than the experimental values causing much larger backward displacement.

No doubt that error is introduced to the results since the solution is obtained without the effects of viscosity. Ejector force approximation could also affect the Euler angles and rates since the correct ejector modeling used in the experiment is not exactly known. Also the time accurate modeling of the flow would result in a different flow field calculation than the quasisteady modeling of the experimental results [5]. Despite all these errors, it can be concluded that the CFD-FASTRAN solver can be used in the store separation problems.

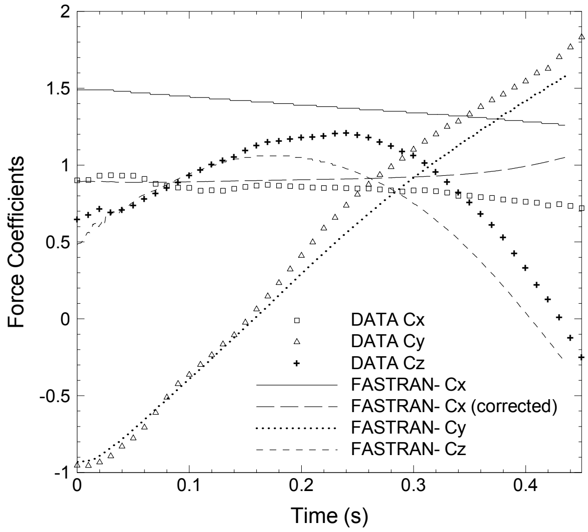

Figure 11: Time History of Force Coefficients on the Store, Eglin Validation Test Case, M=0.95

5.2 Eglin Wing-Pylon-Finned Store Release at M=0.3 and M=0.6

These cases are solved with both the Euler and the panel codes. The aim is to compare the two methods of prediction tools and to find out which aspects of the store separation phenomenon could be captured. The results are given in linear and angular displacements of the store in its trajectory and the pressure distribution on the store in its captive position (t=0 s) right before the separation and the time histories of the force coefficients, acting on the store along its trajectory.

Calculated drag value includes the pressure forces, but excludes the viscous effects in Euler solution. Due to inviscid nature of the flow, base drag value could not be calculated correctly. Panel code gives pressure drag value after the boundary layer coupling; therefore the total drag predicted by the panel/boundary layer method includes the skin friction drag as well. Base wake model is used in USAERO for the flow separation at the base-cut section.

For investigating the effect of base cut and the separated flow, a series of test cases are run with both codes using the configurations given in Figure 12. Mach number is taken as 0.3. The store base is smoothed in order to have a reasonably attached base flow. Base wake model is not used for this case in USAERO solution. The comparison of the resultant force and moment coefficients with the base-cut model (Figure 13) are given in Tables 1 and 2, respectively.

It is observed that smoothing the base of the store reduces the drag value as obtained by the Euler code. This is an expected result since the base drag value is included in the base-cut configuration. However, the reverse effect is observed when the panel code is used. Drag value is reduced when the base wake model is introduced

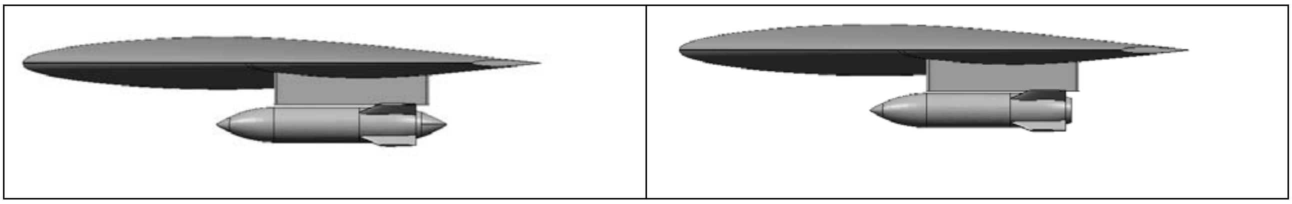

Figure 12: Eglin Configuration with a Smooth Base (left) and Cut Base (right)

Table 1: Force Coefficient Comparison, M=0.3

Case 1	CFx	CFy	CFz	Case 2	CFx	CFy	CFz
FASTRAN	0.214	-0.444	0.511	FASTRAN	0.384	-0.449	0.695
USAERO	0.196	-0.227	0.668	USAERO	0.128	-0.285	0.695

Table 2: Moment Coefficient Comparison, M=0.3

Case 1	CMx	CMy	CMz	Case 2	CMx	CMy	CMz
FASTRAN	0.0945	1.2307	0.1153	FASTRAN	0.0967	1.702	0.1261
USAERO	0.0101	1.3082	0.2099	USAERO	0.0110	1.465	0.0225

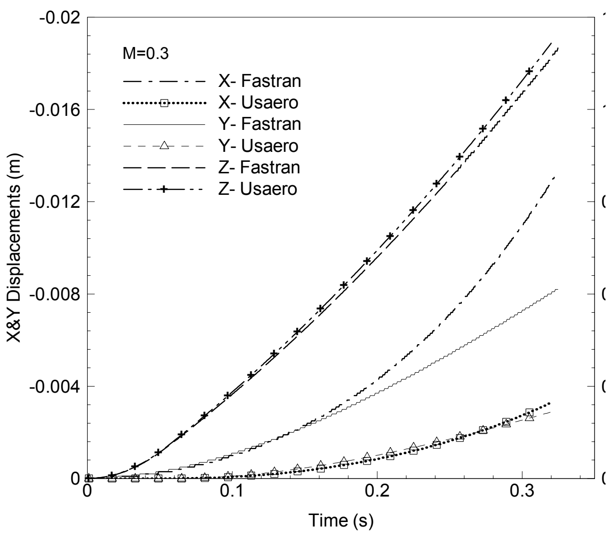

Figure 13: Linear Displacements, M=0.3

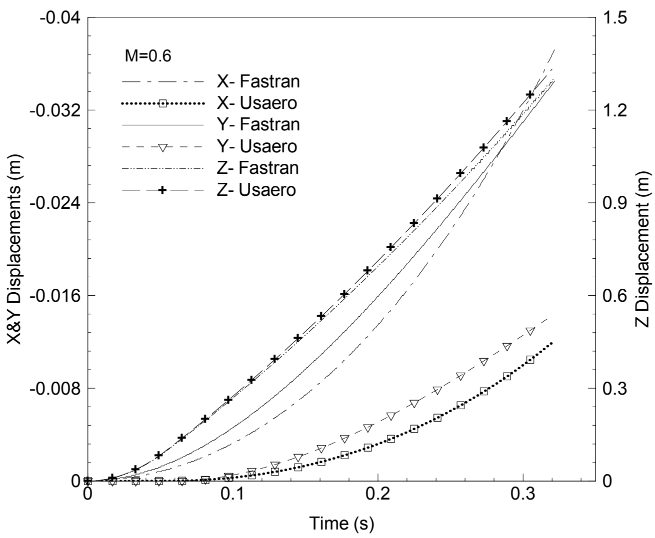

Figure 14: Linear Displacements, M=0.6

Figures 13 and 14 show the linear displacement graphs of the base-cut configuration for M=0.3 and M=0.6, respectively. The X and Y displacements are very small compared to Z displacement. Therefore, a different scale has to be used for Z displacement graphs. The differences in the captive carriage forces are reflected in the X and Y displacements. Although the same trends are captured by both codes, significant discrepancies are observed in the X and Y components. Z displacements give almost the same results for both codes at both Mach numbers. It is observed that the Cfz values calculated with both codes are nearly the same at Mach 0.3.

Angular orientations can be seen in Figures 15 and 16 for Mach 0.3 and 0.6, respectively. Yaw and roll angles have the same trends for USAERO at both Mach numbers. Angles calculated by USAERO and FASTRAN are in close agreement with each other and have similar behaviors at Mach 0.3. However, CFD-FASTRAN calculations performed at Mach 0.6 exhibit a different trend for the pitch angle variations than that predicted by the USAERO. The largest discrepancy is observed in the roll angle predictions by both of the codes at the given Mach numbers, whereas the predictions for the yaw angles by both of the codes are in better agreement. This agreement is getting better with increasing Mach number.

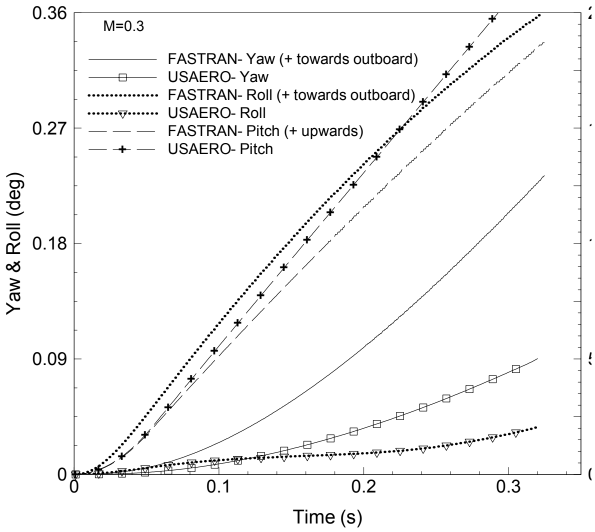

Figure 15: Angular Displacements, Mach 0.3

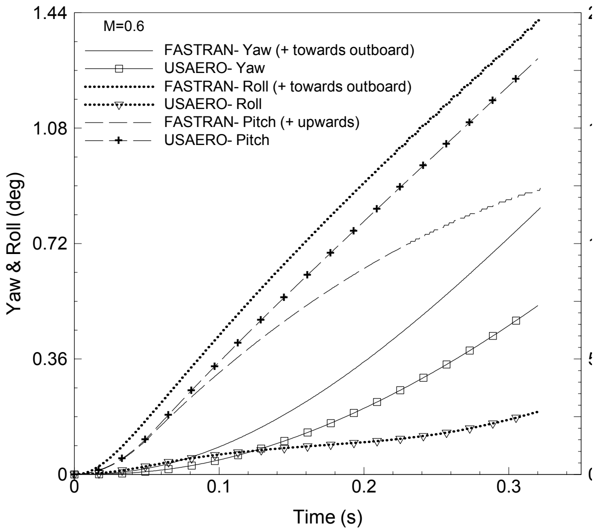

Figure 16: Angular Displacements, Mach 0.6

Pressure distributions on the store in its captive position are drawn at Phi= 0^0, 90^0, 180^0 and 270^0 angle planes and given in Figures 17 and 18. The pressure distributions calculated with both codes have the same trend. Interaction between the pylon and the store can be observed in Euler solution at Phi=0^0, which is the location between the store and the pylon. The same compression is also observed in the panel method but with a much weaker strength.

For Phi=90^0, 180^0 and 270^0 angles, CFD-FASTRAN calculates lower Cp values than the panel code after x/c = 0.75. Same behavior is observed when the Cp distributions are compared with the experimental results in the Eglin case at M=0.95. This difference can be attributed to the nature of the Euler solver which excludes the effects of viscosity. Boundary layer coupling option when introduced to the panel method improves the Cp distributions obtained by the USAERO code. This difference in pressure distribution results in lower force and moment coefficients values than obtained in CFD-FASTRAN.

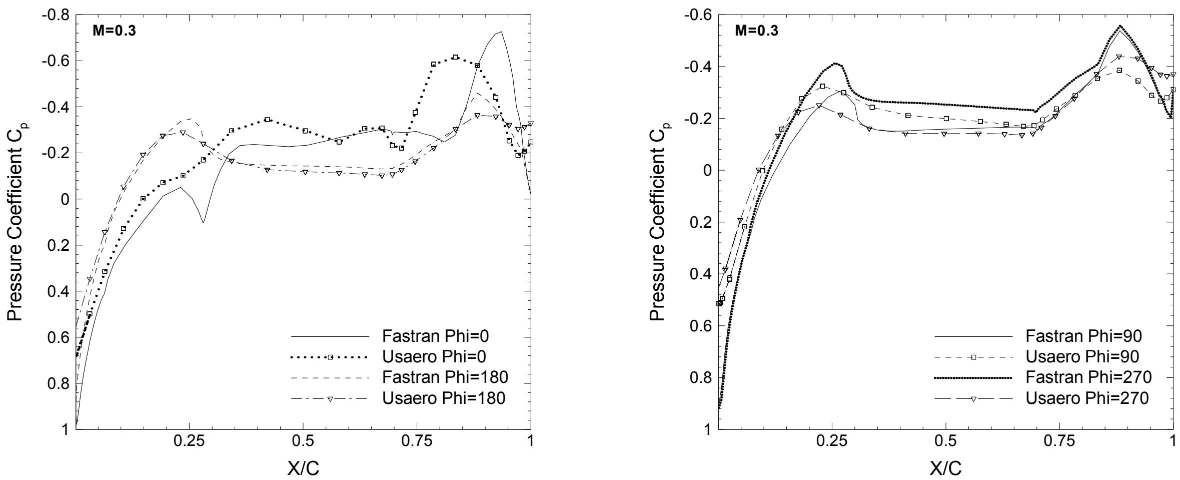

Figure 17: Pressure Distribution on the Store in Captive Position, USAERO and CFD-FASTRAN Results, M=0.3

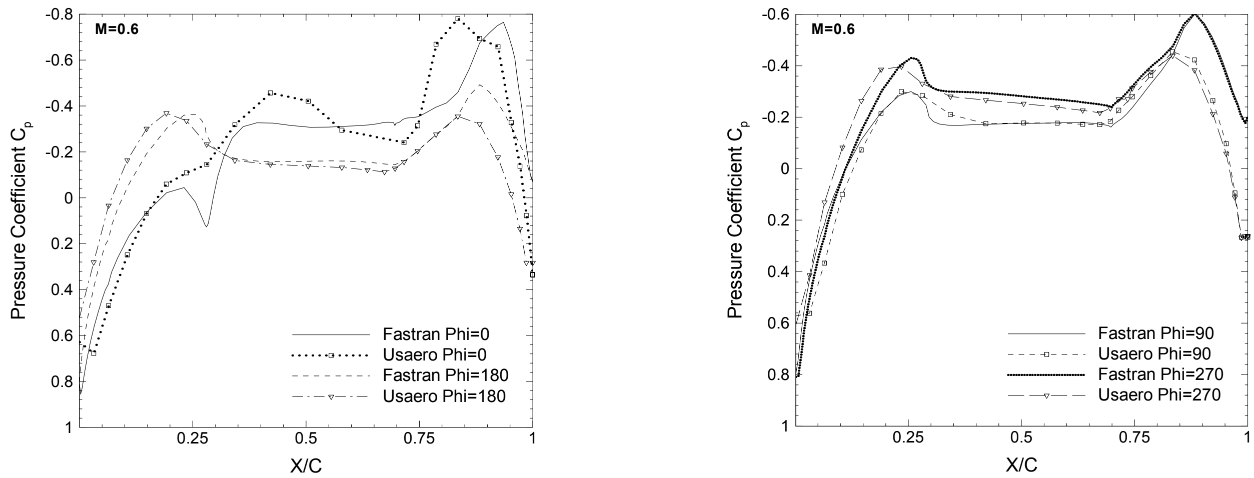

Figure 18: Pressure Distribution on the Store in Captive Position, USAERO and CFD-FASTRAN Results, M=0.6

Time histories of force coefficients are given in Figures 19 and 20 for M=0.3 and M=0.6, respectively. The trends are in better agreement at M=0.6 than M=0.3 results. In particular, CFz and CFy values become very close to each other at t=0.32 seconds, where the store is more than 1 meter away from the wing. Also the pitch angle is almost 13^0 for Euler and 17^0 for the panel code at that location. It is well known that the predictions by both the Euler and the panel codes are not very reliable at high angles of attack. This may be a result to see that both codes have the same error in that case.

A summary of the force and moment coefficients at captive carriage state are given in Table 3.

Since there are no experimental results available for these configurations, the discussions are based on the comparisons of the results of the panel with the Euler codes. The accuracy could be improved after comparison with wind-tunnel test results

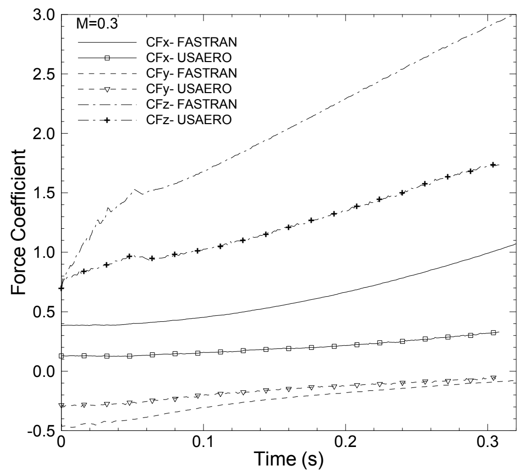

Figure 19: Time Histories of Force Coefficients, M=0.3

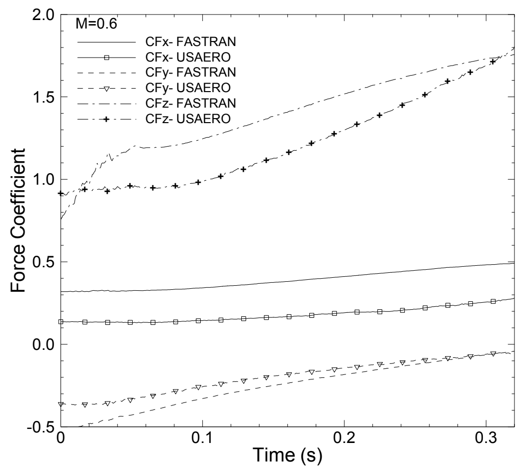

Figure 20: Time Histories of Force Coefficients, M=0.6

Table 3: Force and Moment Coefficients Summary, M=0.3, M=0.6

Eglin Test Case		CFx	CFy	CFz	CMx	CMy	CMz
M=0.3	FASTRAN	0.384	-0.449	0.695	0.0967	1.702	0.1261
	USAERO	0.128	-0.285	0.695	0.0110	1.465	0.0225
M=0.6	FASTRAN	0.319	-0.507	0.758	0.0938	1.839	0.1111
	USAERO	0.137	-0.362	0.912	0.0130	1.882	0.0406

5.3 F-16 Fighter Aircraft Wing Alone / Full Configuration Cases

These cases are solved with only the panel code. The aim is to find out the trajectory of the store and the effect of fuselage on the store separation phenomenon. The results are given in linear and angular displacements of the store in its trajectory and the pressure distribution on the store in its captive position (t=0s) right before the separation and the histories of the force coefficients.

Linear displacement graphs are given in Figure 21. Z displacements for both configurations are almost the same. X displacement for the wing alone configuration has the same trend with the full aircraft configuration, but the drag value is higher (Figure 24). Therefore, the store separated from the wing moves faster backwards when compared with the full aircraft configuration. The most important difference is observed in the Y displacement. The side force calculated on the store in the wing only case is very small when compared with the force obtained for the full aircraft configuration. As a consequence of this side force, an inboard movement of the store is observed in the full aircraft configuration whereas the opposite is true for the wing alone case.

Angular displacement graphs are given in Figure 22. Pitch angle has the same trend for both cases. However, yaw and roll angles have shown opposite behaviors. The store separated from the full aircraft configuration rolls outboard and yaws to inboard whereas the store separated from the wing exhibits opposite angular motions.

Pressure distribution graphs are given in Figure 23. Compression due to the pylon is observed with both configurations at Phi=0^o angle plane. Pressure distributions at Phi=90^0 and Phi=270^0 plane cuts are almost same for wing configuration and it is observed that there is no significant movement of the store in that direction after separation. However, the pressure on the inboard side of the store is lower than that on the outboard side for the full aircraft configuration. Therefore, the store has a movement towards inboard of the wing when separated from the aircraft.

There is a significant difference in side forces as observed in Figure 24. The negative side force on the store released from the full aircraft configuration shows a linear decrease as the store moves downwards. This result shows the predominant effect of including the fuselage to the modeling of a fuel tank separation problem. Also an increase in the lift and a decrease in the drag coefficient acting on the store is observed.

A summary of the force and moment coefficients at the captive carriage state are given in Table 4.

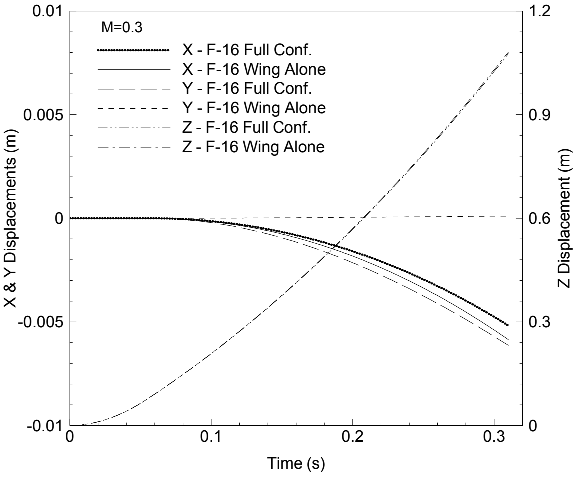

Figure 21: Linear Displacements, Fuel Tank, M=0.3

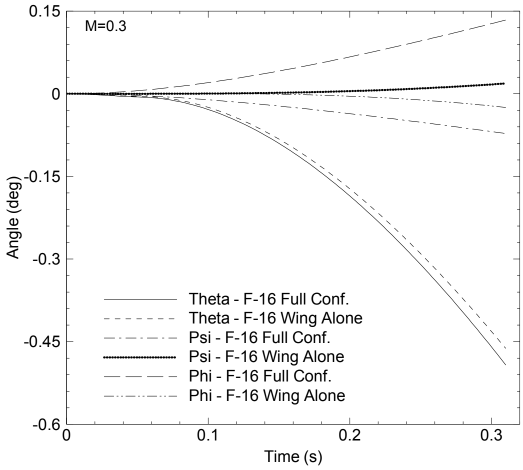

Figure 22: Angular Displacements, Fuel Tank, M=0.3

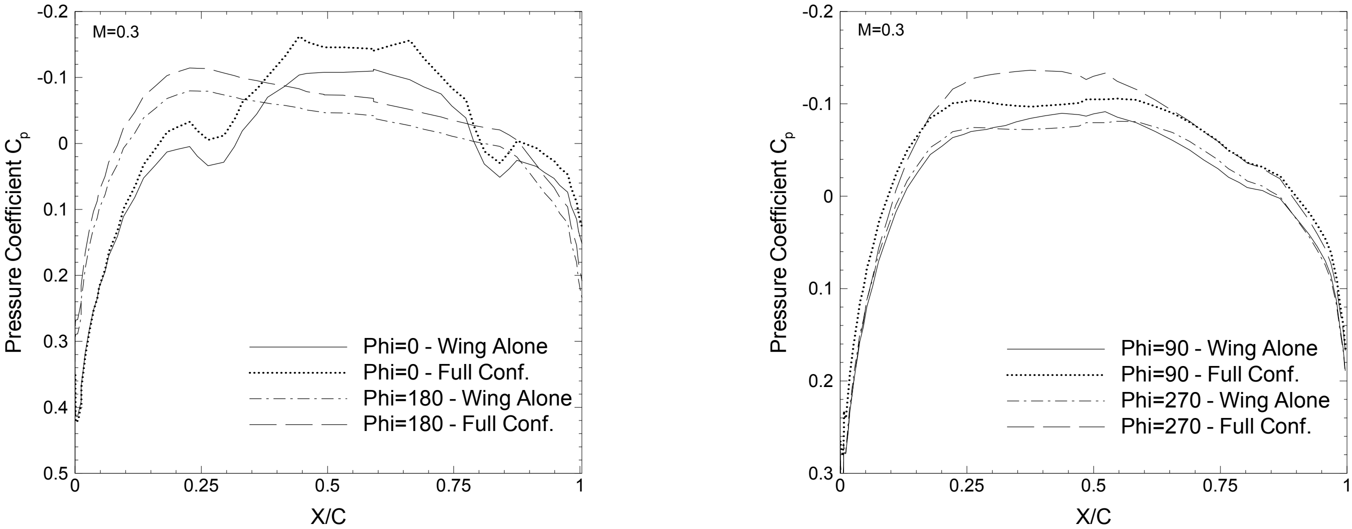

Figure 23: Pressure Distribution on the Fuel Tank in Captive Position, M=0.3

Table 4: Force and Moment Coefficient Summary, M=0.3

Fuel Tank		CFx	CFy	CFz	CMx	CMy	CMz
M=0.3	Wing Conf.	0.0506	0.0044	0.0314	0.0004	-0.7359	-0.0021
	Full Conf.	0.0427	-0.0823	0.0664	0.0034	-0.7585	-0.0517

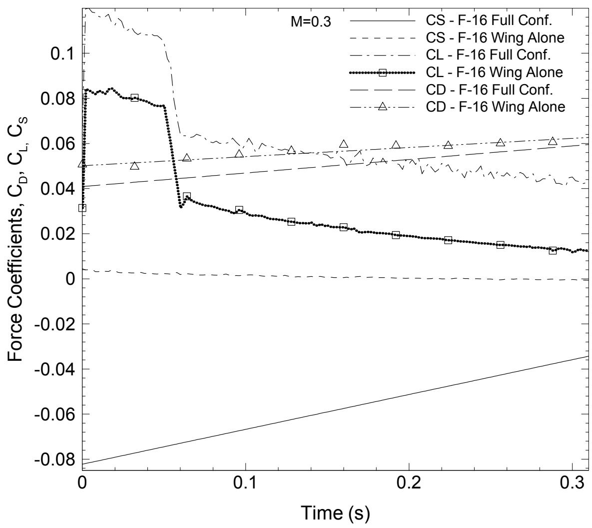

Figure 24: Time Histories of Force Coefficients, M=0.3

6.0 CONCLUSION

In this paper, two different CFD methods are used to obtain the trajectories of a store release problem from 3 different configurations; Eglin test case configuration, F-16 wing-pylon and F-16 full aircraft configurations. Displacements, angular orientations, pressure coefficient distribution on the store in captive position and force coefficient histories during separation are used for comparison purposes.

CFD-FASTRAN, implicit Euler solver is validated against the experimental data of Eglin test case at M=0.95. Same Eglin configuration without the sting attached to the store is used to compare the unsteady panel method with the Euler solution at two different Mach numbers, Mach 0.3 and 0.6. The downward displacements and the pitch attitudes are close to each other for M=0.3. Major trends of the other displacements and angular orientations are similar to each other but the magnitudes have some differences.

The increase in the side force component of the store is observed after comparing the results obtained for the F-16 wing-pylon and full aircraft configurations using USAERO panel code.

Both codes can be used for the aerodynamic design and integration of a new store to an aircraft. Chimera method is well suited to the store separation problems when using Euler solutions. On the other hand, pre-processing and the solution time of the panel code are much less than the Euler code. Therefore, in order to have very fast results for a big test matrix at low subsonic flow conditions, panel code should be preferred. However, Euler solutions must be obtained for the shock dominated flows at transonic flow regimes.

ACKNOWLEDGEMENT

ASELSAN, Technopolis METU, Ankara provided software and hardware support for the realization of USAERO solutions presented in this paper. This support is greatly acknowledged.

REFERENCES

[1] Hall, L.H., Mitchell C.R., Parthasarathy, V., "*An Unsteady Simulation Technique for Missile Guidance and Control Applications,"* AIAA 97-0636, 35th Aerospace Sciences Meeting & Exhibit, January 6-10, 1997 / Reno, NV

[2] Rock, S.G. and Habchi, S.D., Yeiser, C. and Oslon, M., Marquette, T., "*A computational Methodology for the Rapid Simulation of Jettisoned Aircraft Canopy Trajectories,"* AIAA 97-0169, 35th Aerospace Sciences Meeting & Exhibit, January 6-10, 1997 / Reno, NV

[3] Hall L. "*Navier-Stokes/6-DOF Analysis of the JDAM store separation from the F/A-18C Aircraft,*" AIAA Paper 99-0121, January 1999

[4] Chen, P.C., Liu, D.D., "*Store-Separation Analysis at Subsonic and Supersonic Speeds Using a High-Order Panel Method,*" AGARD 76th Fluid Dynamics Panel Meeting and Symposium on Aerodynamics of Store Integration and Separation, Ankara, Turkey, 24-28 April, 1995

[5] Lijewsky, L.E., and Suhs, N.E., "*Time Accurate Computational Fluid Dynamics Approach to Transonic Store Separation Trajectory Prediction,"* Journal of Aircraft, Vol. 31. No.4, pp. 886-891

[6] Prewitt, N.C., Belk, D.M., and Maple, R.C., "*Multiple Body Trajectory Calculations Using the Beggar Code,"* Journal of Aircraft, Vol. 36, No.5, 1999, pp. 802-808

[7] Lee, S., and Park, M., Cho, K.W., Kwon., J.H., "*New Fully Automated Procedure for the Prediction of Store Trajectory,"* Journal of Aircraft, Vol. 37, No.6, November-December 2000

[8] Fox, J.H., "23. *Generic Wing, Pylon and Moving Finned Store," RTO-TR-26, Verification and Validation Data for Computational Unsteady Aerodynamics, October 2000*

[9] Erhan., H., "*Aerodynamic Analysis of Fighter Aircraft F-16 with External Stores,*" MSc. Thesis, 2003, METU

[10] Bozkurttaş, M., "*Aerodynamic Analysis of External Stores on Aircraft*," MSc. Thesis, 2001, METU

[11] USAERO, User's Manual, Version 4.2., 2002 Analytical Methods, INC.